Optimal shape of repair patches in composites

31st Congress of the International Council of the Aeronautical Sciences

Belo Horizonte, Brazil; September 09-14, 2018

OPTIMAL SHAPE OF REPAIR PATCHES IN COMPOSITES

Leonel Echer* , **Carlos Eduardo de Souza**** , **Rogério José Marczak***
***Federal University of Rio Grande do Sul** , ****Federal University of Santa Maria**

Keywords: *Repair patch shape; laminate material; structural optimization; finite element analysis.*

Abstract

In recent decades, the increase in demand for advanced composites in the replacement of conventional materials, to both primary and secondary aircraft components, reached a concerning level. The safety and efficiency of composite aircraft components are significantly dependent on damage assessment and repair techniques. In this scenario, the use of composite repair patches for restoring and/or improving the original strength and stiffness conditions of damaged components is a viable option. This statement is particularly true when replacing the entire damaged component is not cost-effective. The present work proposes an optimization-based methodology for obtaining the best patch configurations for the repair of damaged laminate panels. A two-phase optimization was employed: first, the fiber orientation that maximizes the strength of the repair patch was defined, followed by the minimization of the repair surface. Circular and square repair patch shapes were tested. The parent plate was considered as a rectangular plane laminate with two different stacking sequences, and different boundary conditions were tested as well. The patch was modeled as an unbalanced fiber reinforced repair with a single layer. Linear programming was employed to solve both optimization problems: fiber orientation and shape area. The error concerning the first natural frequencies of the repaired component compared to the damaged one was considered as the objective function.

1 Introduction

The increase of structural applications for advanced composites direct implies in need for efficient manufacturing processes and damage detection techniques. Moreover, as appointed by the US Government Accountability Office (GAO), to sustain the increase in demand for advanced composites at a health state growth level, the development of technology for both structural repair and maintenance operations is mandatory [1]. In the current scenario, where the aerospace industry uses large and highly integrated composite structures, the complete replacement of damaged composite components might not be economically viable. This plot led to the need for sustainable options to extend the life of expensive composite damaged components, under a practice way more demanding than the usual Aluminum/Steel/Titanium parts repair. In this context, fiber-reinforced adhesive patches are, undoubtedly, the most promising and efficient way to restore or even improve the mechanical response of damaged composites [2].

1.1 Fiber Reinforced Repair Patches

The search for repairing techniques by the aerospace sector is not recent. Composite repair patches have been employed by the Australian Research Laboratories (ARL) since the late 1960's [3, 4]. These pioneer works successfully applied repair patches made of BFRP and CFRP to extend the life of cracked metallic components of several military aircraft [5, 6]. Through the following decades, considerable progress has been achieved in the use of bonded

fiber reinforced repair patches. However, there are still several limitations concerning such techniques.

The use of fiber reinforced repair patches applied to damaged composite structures is still very limited, by both aviation rules and certification, and technology development [7]. Usually, only conventional rectangular geometries with predefined fiber orientation and stacking sequences are considered. The vast majority of the existing research of composite repair patches is presented for metallic components [8, 9], mostly cracked plates in which composite patches are applied aiming to reduce the Stress Intensity Factor (SIF) and prevent crack growth. These early works [3–6, 8, 9] usually determined the repair shape by experimentation without seriously considering the material waste and inertia increment caused by the use of oversized patches.

Along the last years, different approaches intended to achieve patches designed to minimize the drawbacks caused by large repair patches [11], such as excessive mass gain, non-aerodynamic surface, residual thermal stress due to curing. Some of the patch shapes proposed in the last years may be listed as:

- Skewed repair patch [10] priming for the material distribution along crack tips.
- Modified skewed repair patch [12] obtained by improving the work of [10] by the use of genetic algorithms.
- Trapezoidal repair patch [13].
- Arrow head and H-shaped patches [11].
- Bow tie patch [14].

In these works and the vast majority of the others presented in the literature, it is suggested the use of patch shapes capable of distributing a more substantial amount of material on the surroundings of a crack tip [2]. Moreover, most of the repair patch shapes proposed in the literature are defined aiming to reduce the SIF solely, which may not be the best strategy. Such approach is only applicable for crack-like damage. This drawback is particularly critical when working with composites because the definition of the repair patch fibers orientation as being perpendicular to the central damage line (or crack normal direction) might not be the orientation of maximal efficiency. To circumvent this problem is one of the primary objectives of the present work.

1.2 Work Overview

The motivation of the present work lies on the need for a tool suitable to define a composite repair patch capable of restoring the stiffness of a damaged component, $\boldsymbol{K}_D$, to its original (undamaged) configuration, $\boldsymbol{K}_0$. Such tool would be suitable for applications of repair and also for local/directional enhancement of mechanical strength. Both purposes are a demand of the aerospace industry with high relevance and applicability. This statement is especially true in recent years when the search for the reduction in weight, fuel consumption and pollutants emission has dramatically changed the total amount of advanced composites employed in aircraft [15].

The present work approaches the use of composite repair patches applied to damaged laminated panels aiming to achieve a repaired component with structural stiffness and inertia as close as possible to its original design. Fig. 1.2 illustrate the concept of the present works main goal: achieve an optimum based repair patch shape.

2 Optimization-Based Repair Patches

The most efficient repair patch must be capable of restoring the original strength of a damaged component, but not at the cost of excessive inertia increment. In order two achieve this condition, the methodology proposed herein incorporates a two-phase optimization formulation. The first one aims an optimal parameter for ply angle, which is employed as an entry for the second optimization. The objectives of both phases are presented, respectively, as:

1st - Define the fibers orientation angle ϕ that maximizes the repair efficiency;
2nd - Obtain a patch geometry that minimizes material usage, patch area A, and restore undamaged response.

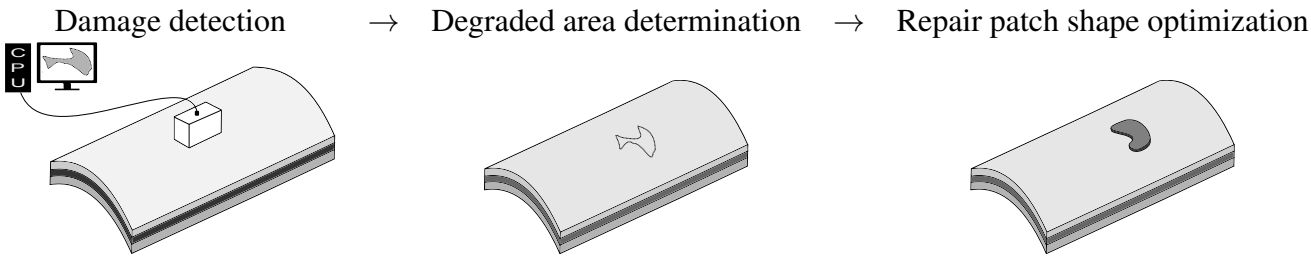

Fig. 1 Logical sequence to achieve an optimally repaired component.

This methodology and the objectives aimed are presented by Fig. 2.

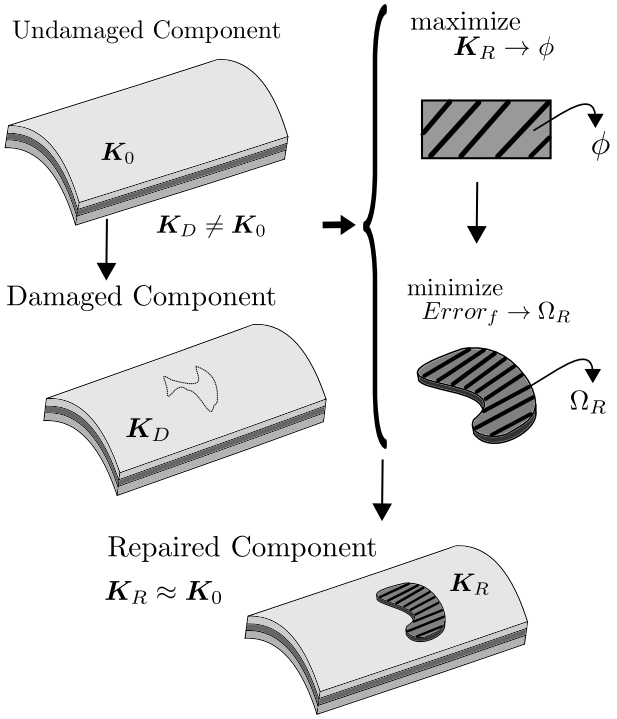

Fig. 2 Repair shape optimization strategy.

2.1 Study Cases

The geometry of study was selected aiming to reproduce the scenario of a composite panel employed in structures such as aircraft fuselage; wing skin; wind turbine blades; among others. These panels are physically attached to its neighbors, leading to two possible boundary conditions, fully clamped (FC) or simply supported (SS). This lead to the definition of a rectangular flat laminate, with dimensions $l \times l/2$, to be considered as parent plate. Two different stacking sequences were analyzed [0/45/-45/90]s and [45/-45/0/90/60/-30/90/-45], both with ply thickness, t_i, equal to 0.4mm. The component was modeled with a central rectangular damage zone, with dimension $d \times d/4$, acting on all layers, fully trespassing, as presented in Fig. 3.

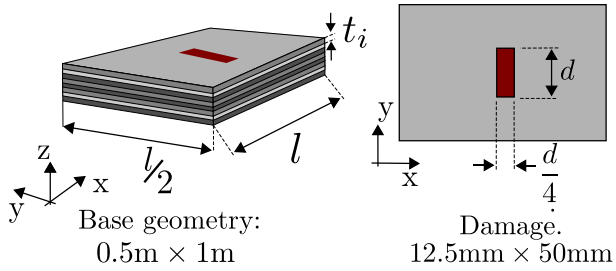

Fig. 3 Geometry of the parent plate.

Two possible repair patch shapes were considered, circular and square. Each geometry counts with two design variables, the fiber orientation angle ϕ and the radius R for the circular patch or side S for the square patch. The repair patch thickness t_r is equal to 0.4mm, which is the same as t_i. These features are illustrated in Fig. 4.

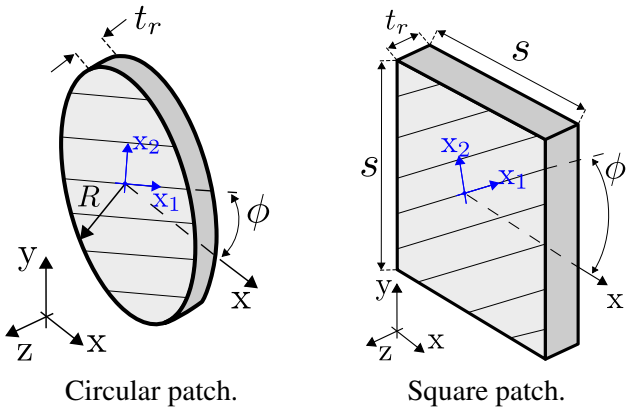

Fig. 4 Repair shapes.

The material was considered as a transversally isotropic CFRP: $E_{11} = 147\text{GPa}; E_{22} = 9.8\text{GPa}, G_{12} = 2.35\text{GPa}; G_{23} = 3.3\text{GPa}, \nu_{12} = 0.405; \nu_{23} = 0.485; \rho = 1580\text{kg/m}^3$. The damage area was modeled by means of local mechanical properties degradation in five orders of magnitude. It must be noted that only the elasticity and shear modulus are affected. The density of the material in the damage area is kept unchanged.

2.2 Optimization Formulation

In the present work, the optimization formulation is presented as the minimization of an objective function $\text{Obj}(x_i)$ subjected to side constraints, g_i and h_i acting over the design variables x_i:

$$\begin{aligned} \underset{x_i}{\text{minimize}} \quad & \text{Obj}(x_i), \\ \text{subjected to} \quad & x_i \leq g_i, \\ & x_i \geq h_i. \end{aligned} \tag{1}$$

The optimization formulation employed herein does not directly evaluate the repaired structures stiffness, $\boldsymbol{K}_R$, instead, a surrogate approach is applied. The modal response of the structure is used as a metric for evaluating the efficiency of the repair patch.

The first optimization problem is the simpler, with ϕ as a single design variable. The objective function is defined in order to maximize first natural frequencies of the repaired structure, f_i. Eq. 2 expresses the resulting optimization problem.

$$\begin{aligned} \underset{\phi}{\text{minimize}} \quad & \text{Obj}_\phi = \sum_{i=1}^{3} \left(\frac{f_i}{\bar{f}_i} \right), \\ \text{subjected to} \quad & -\pi/2 \leq \phi \leq \pi/2 \end{aligned} \tag{2}$$

where, $\bar{f}_i$ corresponds to the first natural frequencies of the undamaged structure, comparison solution, and the side constraints applied over ϕ allows any possible fiber orientation.

After obtaining an optimized value for ϕ, it is employed as an entry data for the second optimization, which aims to achieve the minimum repair patch area capable of restoring the repaired component modal response to its undamaged state. The objective function of this second optimization is the error with respect the first natural frequencies of the comparison solution,

$$Error_f = \sqrt{\sum_{i}^{3} \left(\frac{f_i - \bar{f}_i}{f_i} \right)^2}, \tag{3}$$

and the optimization formulation is expressed as

$$\begin{aligned} \underset{x_i}{\text{minimize}} \quad & Error_f, \\ \text{subjected to} \quad & x_l \leq x_i \leq x_u \quad \forall x_i \in \Omega_R, \end{aligned} \tag{4}$$

where, the side constraints x_l and x_u are the lower and upper limits for x_i, respectively. Also, the feasible domain, Ω_R, of the design variables is defined as the edges of the parent plate.

The coupling of the two-phase optimization process is presented as:

1. Evaluate $\bar{f}_i$, comparison model.
2. Obtain the optimal ϕ:
   (a) Random initial guess for ϕ, iteration $i = 1$.
   (b) Employ a pre-defined repair patch shape and size.
   (c) Build and solve the shell finite element model of the repaired structure.
   (d) Evaluate Obj_ϕ.
   (e) Check convergence.
   (f) If converged go to Step (k)
   (g) Evaluate sensibility.
   (h) Solve linear problem and obtain new parameter ϕ_i.
   (i) Adjust moving limits, α.
   (j) Go back to Step (b).
   (k) Optimal solution for ϕ obtained.
3. Obtain a random initial guess for x_i.
4. Build and solve the shell finite element model of the repaired structure.
5. Evaluate $Error_f$.
6. Check convergence.
7. If converged go to Step 12
8. Evaluate sensibility.

9. Solve linear problem and obtain new design variables x_i.
10. Adjust moving limits, α.
11. Go back to Step (4).
12. Optimal solution obtained.

Each repair shape was submitted to the proposed optimization methodology. For each case, the objective function was linearized employing Taylor Series expansion. The associated linear problems were solved using Linear Programming, LP, [16] and an interior point algorithm [18]. Forward finite differences was used to evaluate the sensitivity of the design variables. The updating of the moving limits was performed using a heuristic based on past iterations history [17].

3 Results

In the following sections, the term FC is employed to refer to the study cases with Fully Clamped boundary conditions. Analogously, the term SS is equivalent to Simple Supported boundary conditions.

3.1 Optimized Fibers Orientation ϕ

The optimal ϕ for each case of study is presented in Tab. 1 and Tab 2. The number of iterations until convergence and the initial random guess for each optimization problem are presented as well.

Table 1 Laminate [0/45/-45/90]s

	FC	SS
Iterations until convergence	25	25
Initial guess, ϕ_1	$-33.23°$	$32.80°$
ϕ_{otim}	$-3.15°$	$-6.02°$

Table 2 Laminate [45/-45/0/90/60/-30/90/-45]

	FC	SS
Iterations until convergence	18	27
Initial guess, ϕ_1	$36.43°$	$80.30°$
ϕ_{otim}	$32.16°$	$13.69°$

In none of the analyzed cases, the optimized fiber orientation angle was perpendicular to the damage neutral axis (damage length). Although of being primarily used in the literature, and being accepted for the repair of cracked metallic plates, this approach is inappropriate in the study of composites. Besides, the definition of the repair patch orientation is not trivial even for simple and symmetric stacking sequences. Concerning the restoring of damaged repair patches, an optimum-based methodology for the definition of ϕ appears to be the best answer.

3.2 Optimized Repair Patch Shapes

In the following subsections, the optimized repair shapes obtained for all study cases are presented in terms of optimized design variables, R and S, and area of the optimized configuration, A_c for the circular patch and A_s for the square patch. Once more, the term FC is employed to refer to Fully Clamped boundary conditions, and the term SS is equivalent to Simple Supported.

3.2.1 Laminate [0/45/-45/90]s

The optimized configuration for the circular repair patch is presented in Figs. 5 and 6 for the FC boundary conditions. Fig. 5 presents the evolution of the design variable R and objective function $Error_f$ through the optimization process.

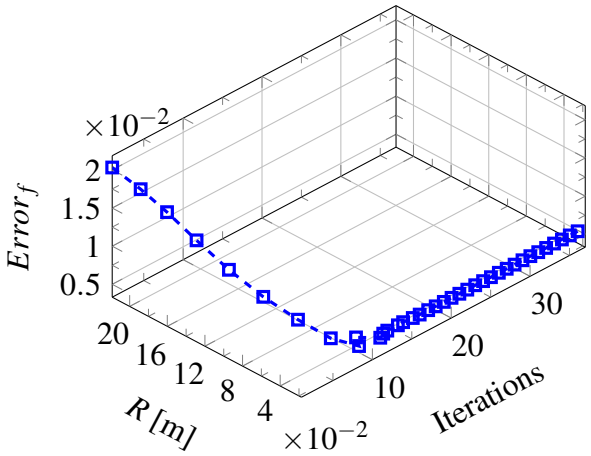

Fig. 5 Circular repair patch: Convergence and optimization evolution - FC.

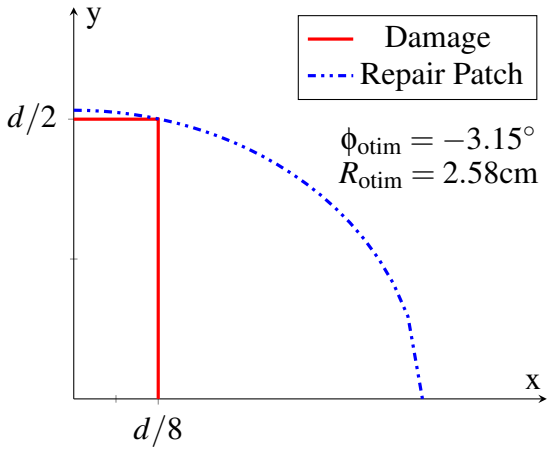

Fig. 6 Circular repair patch: Optimized configuration - FC, showing 1/4 symmetry.

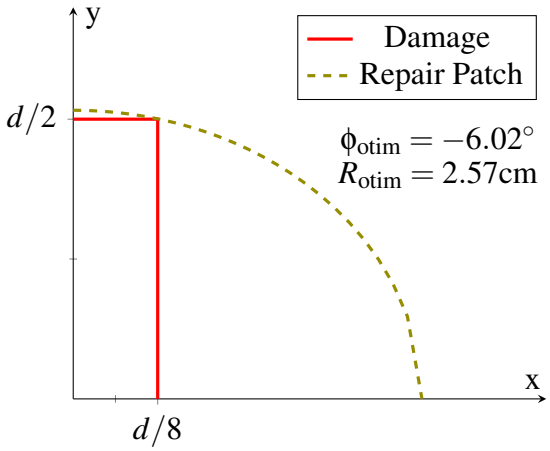

Fig. 8 Circular repair patch: Optimized configuration - SS, showing 1/4 symmetry.

The circular repair shape that minimizes the objective function has a total area equal to $A_c = 20.92\text{cm}^2$ and $R = 2.58\text{cm}$. The configuration of Fig. 5 was obtained after 37 iterations. One must note that the optimized repair patch minimally covers the edges of the damaged area. Moreover, the result presented by Fig. 5 indicates a smooth convergence behavior.

Figs. 7 and 8 presents the optimized solution of the circular repair patch for the SS boundary conditions.

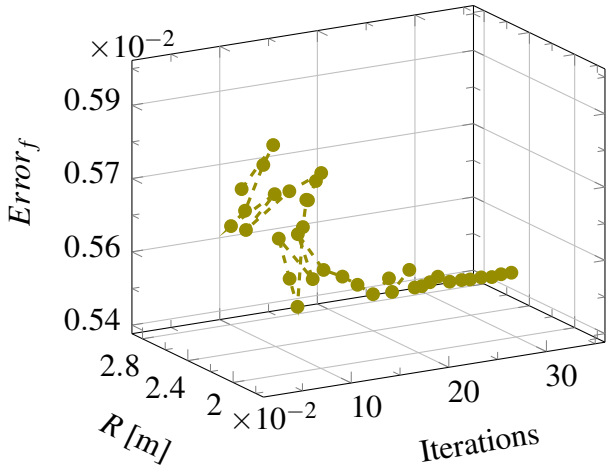

Fig. 7 Circular repair patch: Convergence and optimization evolution - SS

The optimized configuration of Fig. 8 has a total area equal to $A_c = 20.90\text{cm}^2$ and $R = 2.57\text{cm}$. The configuration of Fig. 5 was obtained after 36 iterations.

The difference in the solutions obtained for the SS and FC scenarios was minimal. This indicates that despite different boundary conditions, the modal response was similar for both cases.

The optimized configuration for the square repair patch is presented in Figs. 9 and 10 for the FC boundary conditions. Fig. 9 presents the evolution of the design variable S and objective function $Error_f$ through the optimization process.

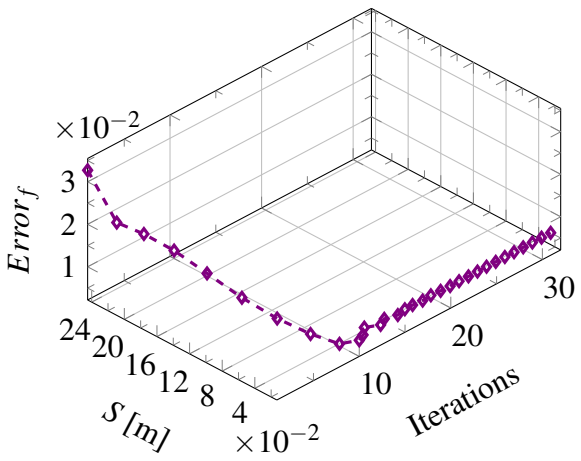

Fig. 9 Square repair patch: Convergence and optimization evolution - FC.

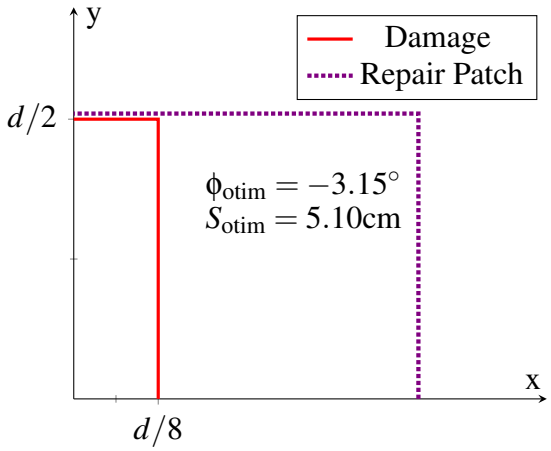

Fig. 10 Square repair patch: Optimized configuration - FC, showing 1/4 symmetry.

The square repair shape that minimizes the objective function has a total area equal to $A_s = 26.01\text{cm}^2$ and $S = 5.10\text{cm}$. The configuration of Fig. 7 was obtained after 32 iterations. The optimized solution for the square repair patch is similar to the one obtained with a circular patch, both in dimensions and total area.

Figs. 11 and 12 presents the optimized solution of the square repair patch for the SS boundary conditions.

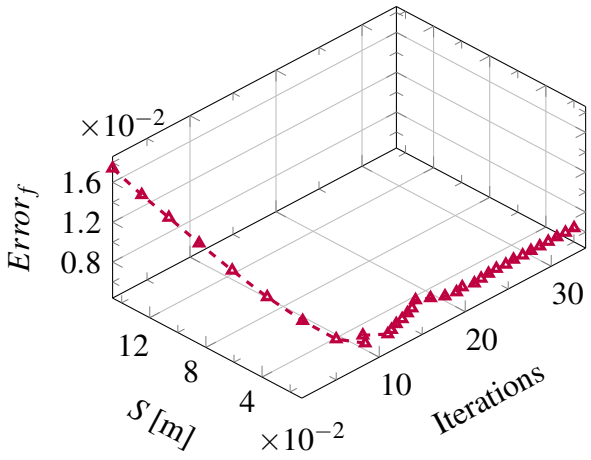

Fig. 11 Square repair patch: Convergence and optimization evolution - SS

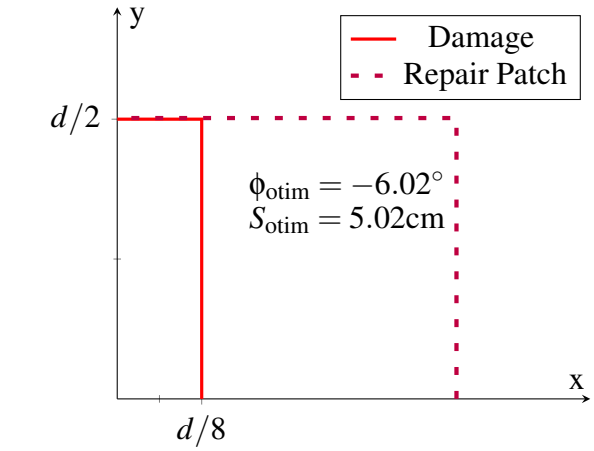

Fig. 12 Square repair patch: Optimized configuration - SS, showing 1/4 symmetry.

The optimized configuration of Fig. 12 has a total area equal to $A_s = 25.02\text{cm}^2$ and $S = 5.02\text{cm}$. The configuration of Fig. 11 was obtained after 34 iterations.

The difference in the solutions obtained for the SS and FC scenarios was minimal. This indicates that despite different boundary conditions, the modal response was similar for both cases.

3.2.2 Laminate [45/-45/0/90/60/-30/90/-45]

Analogously to the previous subsection, the optimized configuration for the circular repair patch is presented in Figs. 13 and 14 for the FC boundary conditions. Fig. 13 presents the evolution of the design variable R and objective function $Error_f$ through the optimization process.

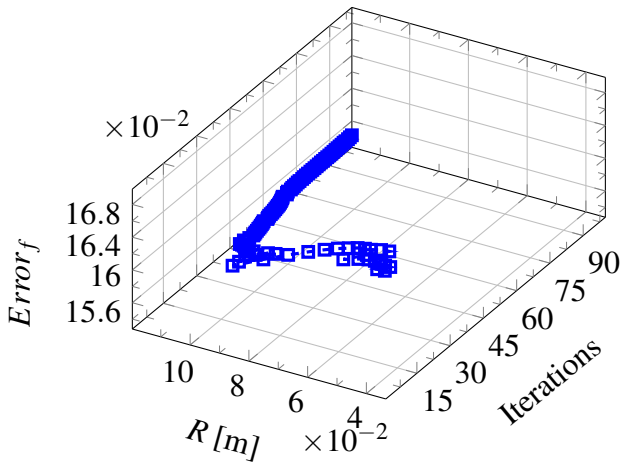

Fig. 13 Circular repair patch: Convergence and optimization evolution - FC.

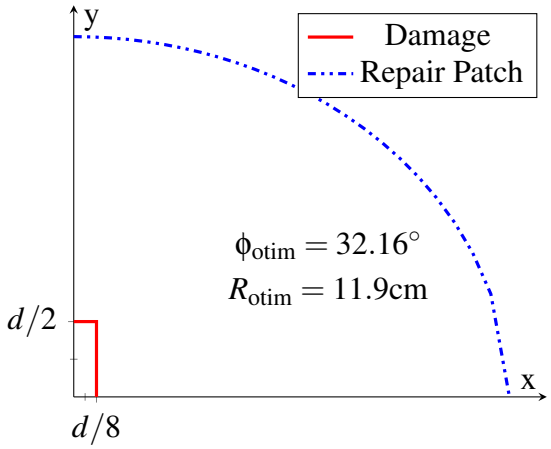

Fig. 14 Circular repair patch: Optimized configuration - FC, showing 1/4 symmetry.

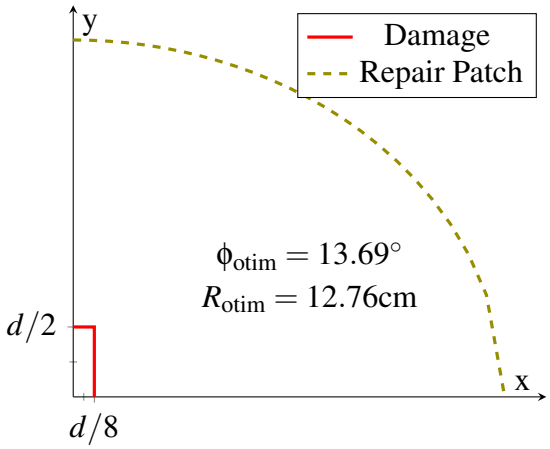

Fig. 16 Circular repair patch: Optimized configuration - SS, showing 1/4 symmetry.

The circular repair shape that minimizes the objective function has a total area equal to $A_c = 449.4\text{cm}^2$ and $R = 11.96\text{cm}$. The configuration of Fig. 13 was obtained after 100 iterations. For the analyzed stacking sequence a larger repair patch was needed in order to restore the structures modal response.

Figs. 15 and 16 presents the optimized solution of the circular repair patch for the SS boundary conditions.

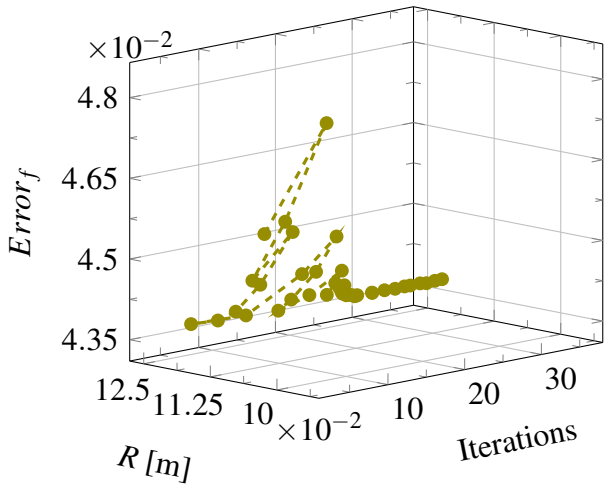

Fig. 15 Circular repair patch: Convergence and optimization evolution - SS

The optimized configuration of Fig. 16 has a total area equal to $A_c = 511.8\text{cm}^2$ and $R = 12.76\text{cm}$. The configuration of Fig. 13 was obtained after 38 iterations.

Similarly to the results obtained for the previous stacking sequence, the difference in the solutions obtained for the SS and FC scenarios was minimal.

The optimized configuration for the square repair patch is presented in Figs. 17 and 18 for the FC boundary conditions. Fig. 17 presents the evolution of the design variable S and objective function $Error_f$ through the optimization process.

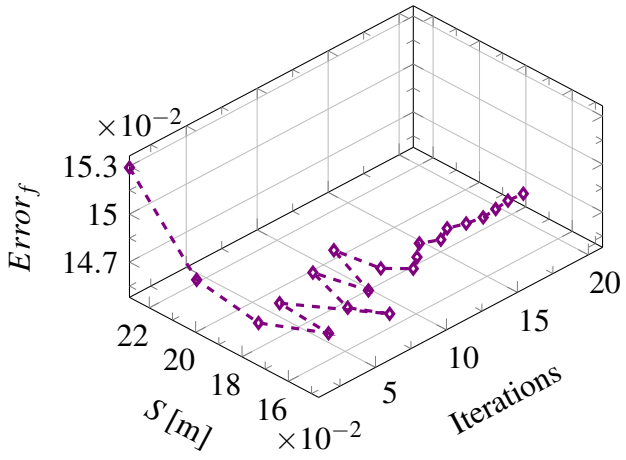

Fig. 17 Square repair patch: Convergence and optimization evolution - FC.

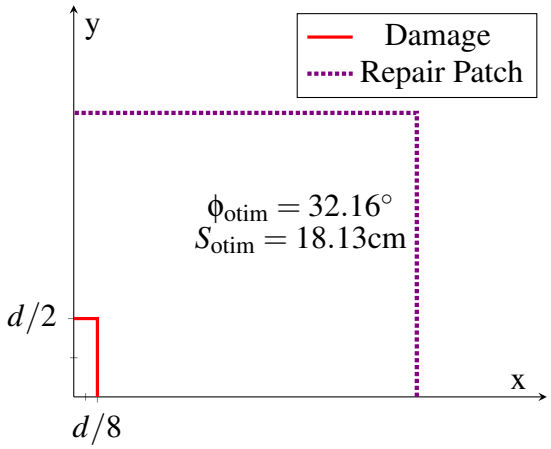

Fig. 18 Square repair patch: Optimized configuration - FC, showing 1/4 symmetry.

The square repair shape that minimizes the objective function has a total area equal to $A_s = 328.54\text{cm}^2$ and $S = 18.13\text{cm}$. The configuration of Fig. 15 was obtained after 21 iterations. Once more, a larger repair patch area was need to restore the modal response to its undamaged condition.

Figs. 19 and 20 presents the optimized solution of the square repair patch for the SS case.

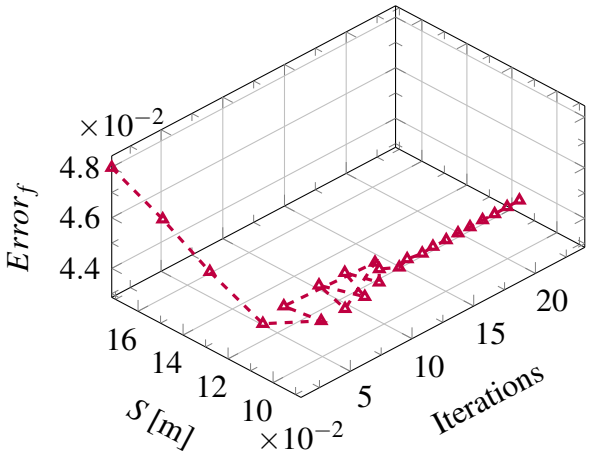

Fig. 19 Square repair patch: Convergence and optimization evolution - SS

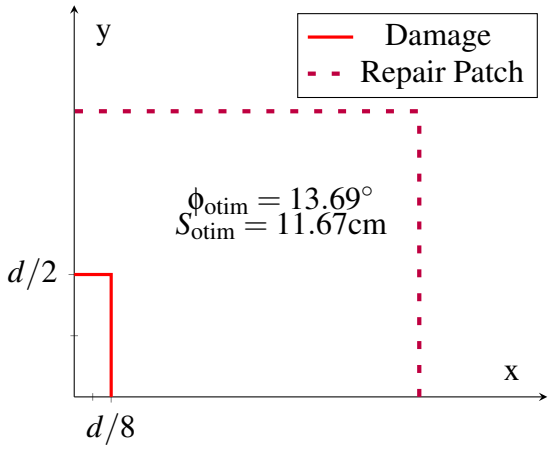

Fig. 20 Square repair patch: Optimized configuration - SS, showing 1/4 symmetry.

The optimized configuration of Fig. 20 has a total area equal to $A_s = 136.18\text{cm}^2$ and $S = 11.67\text{cm}$. The configuration of Fig. 19 was obtained after 24 iterations.

Analogously to the symmetric stacking sequence, the difference in the solutions obtained for the SS and FC scenarios was minimal. This indicates that despite different boundary conditions, the modal response was similar for both cases. This may denote that the optimized repair patch shape is affected by the stacking sequence more than it is affected by the boundary conditions.

4 Final Remarks

The major contribution of the present work is the confirmation that an arbitrary definition of ϕ, perpendicular to the middle line of the damage region, is not efficient. Furthermore, the evaluation of ϕ by means of an optimization procedure allows maximum benefit from the fiber reinforced repair patch. Moreover, the optimized repair shape depends on both parent plate stacking sequence and boundary conditions. However, the influence of the parent plate stacking sequence seems to be far more significant.

References

[1] GAO - US Government Accountability of Office *Aiation Safety: Status of FAA's Actions to*

Oversee the Safety of Composite Airplanes. Report: GAO-11-849, 2011.

[2] Katnam KB, Da Silva LFM and Young, TM. Bonded repair of composite aircraft structures: A review of scientific challenges and opportunities. *Composites Part B: Engineering*, Vol. 53, No. 1, pp 46-61, 2013.

[3] Baker AA. A summary of work on applications of advanced fibre composites at the Aeronautical Research Laboratories, Australia. *Composites*, Vol. 9, No. 1, pp 11-16, 1978.

[4] Baker AA. Repair of cracked or defective metallic aircraft components with advanced fibre composites - an overview of Australian work. *Composite Structures*, Vol. 2, No. 2, pp 153-181, 1984.

[5] Baker AA, Callinan RJ, Davis MJ, Jones R and Williams JG. Repair of Mirage III aircraft using the BFRP crack-patching technique. *Theoretical and Applied Fracture Mechanics*, Vol. 2, No. 1, pp 1-15, 1984.

[6] Baker AA. Fibre composite repair of cracked metallic aircraft components - practical and basic aspects. *Composites*, Vol. 18, No. 4, pp 293-308, 1987.

[7] Baker AA, Andrew JG and Wang J. On the Certification of Bonded Repairs to Primary Composite Aircraft Components. *The Journal of Adhesion*, Vol. 91, No. 1-2, pp 4-38, 2015.

[8] Baker AA and Jones R. *Bonded Repair of Aircraft Structures*. 1st edition, Martinus Nijhoff Publishers, 1988.

[9] Baker AA. Bonded composite repair of fatigue-cracked primary aircraft structure. *Composite Structures*, Vol. 47, No. 1, pp 431-443, 1999.

[10] Kumar AM and Hakeem SA. Optimum design of symmetric composite patch repair to centre cracked metallic sheet. *Composite Structures*, Vol. 49, No. 3, pp 285-292, 2000.

[11] Rachid M, Serier B, Bouiadjra BB and Belhouari M. Numerical analysis of the patch shape effects on the performances of bonded composite repair in aircraft structures. *Composites Part B: Engineering*, Vol. 43, No. 2, pp 391-397, 2012.

[12] Brighenti R, Carpinteri A and Vantadori S. A genetic algorithm applied to optimisation of patch repairs for cracked plates. *Computer Methods in Applied Mechanics and Engineering*, Vol. 196, No. 1, pp 466-475, 2006.

[13] Bouiadjra BB, Bouanani MF, Albedah A, Benyahia F and Es-Saheb M. Comparison between rectangular and trapezoidal bonded composite repairs in aircraft structures: a numerical analysis. *Materials & Design*, Vol. 32, No. 6, pp 3161-3166, 2011.

[14] Bouchiba MSE and Serier B. A step towards the optimization of composite bonded repair shape using an estimation distribution approach. *Journal of the Brazilian Society of Mechanical Sciences and Engineering*, Vol. 39, No. 5, pp 1755-1771, 2017.

[15] Smith F. The Use of Composites in Aerospace: Past, Present, and Future Challenges. *Avalon Consultancy Services ltd*, 2003.

[16] Dantzig GB and Thapa MN. *Linear Programming 2: Theory and Extensions*. 1st edition, Springer, 2003.

[17] Fonseca JSO. *Design of Microstructures of Periodic Composite Materials*. PhD thesis, The University of Michigan, 1997.

[18] Nocedal J, and Wright S. *Numerical Optimization*. 3rd edition, Springer, 2006.

Contact Author Email Address

mailto: leonel.echer@ufrgs.br

Disclosure Statement

No potential conflict of interest was reported by the authors.

Copyright Statement